

# Supramolecular Gold Stripping from Activated Carbon Using $\alpha$ -Cyclodextrin

Wenqi Liu, Leighton O. Jones, Huang Wu, Charlotte L. Stern, Rebecca A. Sponenborg, George C. Schatz, and J. Fraser Stoddart\*



Cite This: *J. Am. Chem. Soc.* 2021, 143, 1984–1992



Read Online

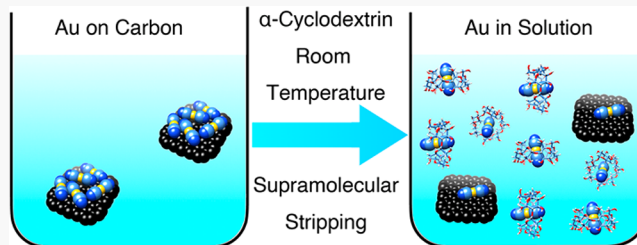
ACCESS |

Metrics & More

Article Recommendations

Supporting Information

**ABSTRACT:** We report the molecular recognition of the  $\text{Au}(\text{CN})_2^-$  anion, a crucial intermediate in today's gold mining industry, by  $\alpha$ -cyclodextrin. Three X-ray single-crystal superstructures— $\text{KAu}(\text{CN})_2\subset\alpha$ -cyclodextrin,  $\text{KAu}(\text{CN})_2\subset(\alpha\text{-cyclodextrin})_2$ , and  $\text{KAg}(\text{CN})_2\subset(\alpha\text{-cyclodextrin})_2$ —demonstrate that the binding cavity of  $\alpha$ -cyclodextrin is a good fit for metal-coordination complexes, such as  $\text{Au}(\text{CN})_2^-$  and  $\text{Ag}(\text{CN})_2^-$  with linear geometries, while the  $\text{K}^+$  ions fulfill the role of linking  $\alpha$ -cyclodextrin tori together as a result of  $[\text{K}^+\cdots\text{O}]$  ion–dipole interactions. A 1:1 binding stoichiometry between  $\text{Au}(\text{CN})_2^-$  and  $\alpha$ -cyclodextrin in aqueous solution, revealed by  $^1\text{H}$  NMR titrations, has produced binding constants in the order of  $10^4 \text{ M}^{-1}$ . Isothermal calorimetry titrations indicate that this molecular recognition is driven by a favorable enthalpy change overcoming a small entropic penalty. The adduct formation of  $\text{KAu}(\text{CN})_2\subset\alpha$ -cyclodextrin in aqueous solution is sustained by multiple  $[\text{C–H}\cdots\pi]$  and  $[\text{C–H}\cdots\text{anion}]$  interactions in addition to hydrophobic effects. The molecular recognition has also been investigated by DFT calculations, which suggest that the 2:1 binding stoichiometry between  $\alpha$ -cyclodextrin and  $\text{Au}(\text{CN})_2^-$  is favored in the presence of ethanol. We have demonstrated that this molecular recognition process between  $\alpha$ -cyclodextrin and  $\text{KAu}(\text{CN})_2$  can be applied to the stripping of gold from the surface of activated carbon at room temperature. Moreover, this stripping process is selective for  $\text{Au}(\text{CN})_2^-$  in the presence of  $\text{Ag}(\text{CN})_2^-$ , which has a lower binding affinity toward  $\alpha$ -cyclodextrin. This molecular recognition process could, in principle, be integrated into commercial gold-mining protocols and lead to significantly reduced costs, energy consumption, and environmental impact.



## INTRODUCTION

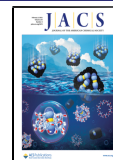
Gold, as a precious metal, is used<sup>1,2</sup> not only in jewelry and currency but also as an increasingly indispensable element in chemical synthesis,<sup>3–10</sup> nanotechnology,<sup>11–14</sup> modern electronics,<sup>15,16</sup> and medicine.<sup>17–19</sup> The recovery<sup>20–24</sup> of gold from ores and electronic waste has become an increasingly active field of research, largely because of economic incentives. One of the most commercially successful processes<sup>1</sup> for gold mining from ores is heap leaching, where alkaline cyanide lixivants are used to solubilize gold as its dicyanoaurate salts,  $\text{NaAu}(\text{CN})_2$  or  $\text{KAu}(\text{CN})_2$ . Activated carbon is introduced to separate the dissolved dicyanoaurate salts from the leached pulps—a technology known<sup>25,26</sup> as carbon in pulp. The dicyanoaurate salts are stripped subsequently from the activated carbon, producing a concentrated solution for the final gold recovery by so-called electrowinning.<sup>1</sup> To strip the dicyanoaurate salts from the activated carbon, harsh conditions,<sup>27–30</sup> including high temperatures (95–140 °C), high pressures (70–400 kbar), and concentrated cyanide and hydroxide solutions, are required. We envision that if the gold-stripping process can be performed at room temperature under mild conditions using nontoxic reagents, a significant

drop in energy consumption, as well as reduced costs and environmental impacts, can be realized.

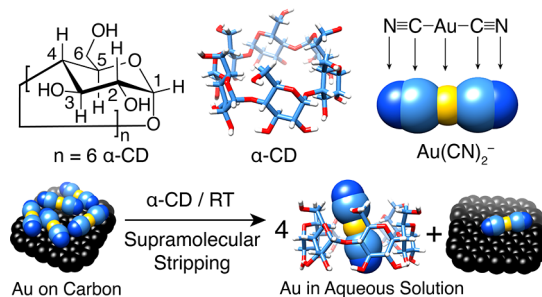
To achieve room-temperature stripping of gold, we hypothesized that a molecular receptor for  $\text{Au}(\text{CN})_2^-$  in aqueous solution might facilitate (Scheme 1) gold transfer from the surface of activated carbon into solution. There are several reports of molecular receptors for gold halide anions relying on the use of cyclodextrins,<sup>31,32</sup> crown ethers,<sup>33</sup> cucurbiturils,<sup>34–36</sup> amides,<sup>37–43</sup> cationic cyclophanes,<sup>44</sup> and metal–organic frameworks,<sup>45–50</sup> which either form precipitates selectively with gold ions or function as gold extraction agents. Anion recognition<sup>51–65</sup> has witnessed a blossoming during the past two decades, where strong binding affinities and high selectivities have been achieved for a wide range of anions. Molecular recognition of  $\text{Au}(\text{CN})_2^-$ , the most relevant anion

Received: November 9, 2020

Published: December 30, 2020



**Scheme 1. Structural Formula of  $\alpha$ -CD with Numerical Labels, a Tubular Representation of  $\alpha$ -CD, a Space-Filling Representation of  $\text{Au}(\text{CN})_2^-$ , and a Graphical Illustration of Gold Stripping from the Surface of Activated Carbon into Aqueous Solution Using  $\alpha$ -CD<sup>a</sup>**



<sup>a</sup>C = light blue, N = dark blue, and Au = golden yellow.

in the gold-mining industry, however, has been explored<sup>66–72</sup> hardly if at all. There are only three reported molecular receptors for  $\text{Au}(\text{CN})_2^-$  using metal–organic cages<sup>69,70</sup> or biotin[6]uril.<sup>72</sup> There are no reports of molecular receptors for  $\text{Au}(\text{CN})_2^-$ , to our knowledge, within the context of commercial gold recovery. The first aim of the present research was to identify molecular receptors for  $\text{Au}(\text{CN})_2^-$  in aqueous solution with the ultimate goal of achieving efficient gold stripping from the surface of activated carbon at room temperature.

Research on cyclodextrins<sup>73–76</sup> has been of particular interest to us.<sup>77–79</sup> Not so long ago, we demonstrated<sup>31,32</sup> that  $\alpha$ -cyclodextrin ( $\alpha$ -CD) can encapsulate tetrabromoaurate in the presence of potassium ions, resulting in selective precipitation of a gold adduct, leading to a green gold-recovery technology. It is also well-known<sup>80–82</sup> that  $\alpha$ -CD can encapsulate selectively substrates with a linear geometry, such as poly(ethylene glycol)<sup>80</sup> and polyiodide complexes.<sup>81,82</sup>

The linear geometry of  $\text{Au}(\text{CN})_2^-$  suggests that this substrate could be a good fit inside the cavity of  $\alpha$ -CD. Herein, we report the molecular recognition of  $\text{Au}(\text{CN})_2^-$ , a critical intermediate in today's gold-mining industry, using  $\alpha$ -CD in water with a binding affinity on the order of  $10^4 \text{ M}^{-1}$ . The binding mechanism has been investigated extensively by using X-ray crystallography, <sup>1</sup>H NMR titrations, isothermal calorimetry titrations, and density functional theory (DFT) calculations. In proof-of-principle investigations, we have demonstrated that this anion-recognition process can be applied to strip  $\text{KAu}(\text{CN})_2$  from the surface of activated carbon at room temperature. We also describe a selective stripping process for  $\text{KAu}(\text{CN})_2$  in the presence of  $\text{KAg}(\text{CN})_2$ , which has a lower binding affinity with  $\alpha$ -CD. With further optimization, this process could be integrated into present gold-mining protocols and lead to significantly reduced costs, energy consumption, and environmental impact.

## RESULTS AND DISCUSSION

Single crystals of a 1:1 adduct were obtained<sup>83</sup> by slow evaporation of an aqueous solution containing a mixture of  $\alpha$ -CD and  $\text{KAu}(\text{CN})_2$ . The solid-state superstructure of the 1:1 adduct between  $\alpha$ -CD and  $\text{Au}(\text{CN})_2^-$  is illustrated in Figure 1. The  $\text{Au}(\text{CN})_2^-$ , which is encapsulated (Figure 1a,b) inside  $\alpha$ -CD, is tilted by about  $14^\circ$  relative to its principal axis. Because the length (9.6 Å) of  $\text{Au}(\text{CN})_2^-$  is slightly longer than the depth (7.9 Å) of the binding cavity, one of the cyanide ligands protrudes outside the primary face of  $\alpha$ -CD. Five of the H-5 protons in  $\alpha$ -CD are in close contact with the Au atom. The [Au…C-5] distances are in the range 4.0–4.3 Å. One of the H-3 protons in  $\alpha$ -CD is in close contact with a cyanide carbon, [N≡C…C-3] distance: 4.1 Å. Two of the H-3 protons in  $\alpha$ -CD have close contacts with the cyanide nitrogens, [C≡N…C-3] distances: 3.9 and 4.4 Å. These short distances (Table 1 and Table S1) suggest that the supramolecular adduct  $\text{Au}(\text{CN})_2^- \subset \alpha$ -CD is sustained by multiple [C–H…π]<sup>84–86</sup>

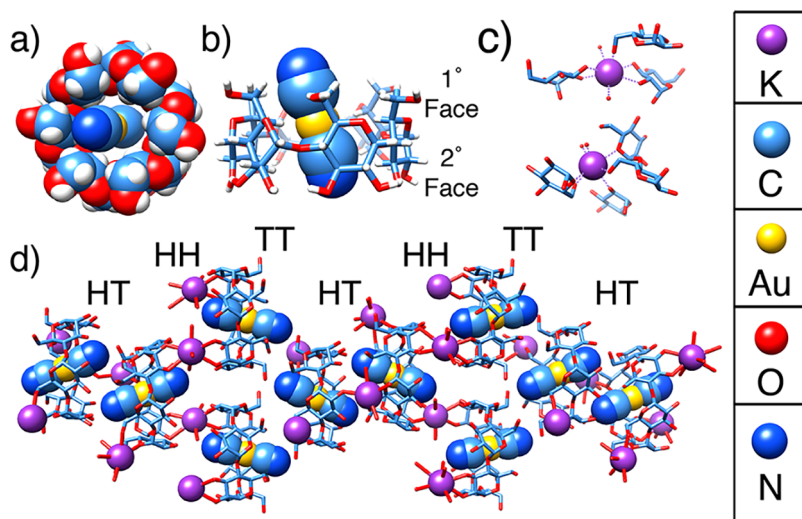


**Figure 1.** Space-filling (a) and tubular (b) representations of the solid-state superstructures of  $\text{Au}(\text{CN})_2^- \subset \alpha$ -CD obtained from single-crystal X-ray diffraction studies. The inward-facing H-3, H-5, and H-6 protons of  $\alpha$ -CD are directed toward the  $\text{Au}(\text{CN})_2^-$  anion, establishing multiple [C–H…π] and [C–H…anion] interactions that stabilize the adduct. (c) Tubular and space-filling representations of two types of  $\text{K}^+$  ions, forming seven  $[\text{K}^+ \cdots \text{O}]$  coordinative bonds with glucose residues and two water molecules with a capped trigonal prismatic coordination geometry. The  $\text{K}^+$  ions are located on both the primary and secondary faces of  $\alpha$ -CD. Each  $\text{K}^+$  ion connects three  $\alpha$ -CDs together. (d) Tubular ( $\alpha$ -CD) and space-filling ( $\text{KAu}(\text{CN})_2$ ) representations of the crystal packing between  $\text{Au}(\text{CN})_2^-$  anions and  $\alpha$ -CDs, showing the positions of  $\text{K}^+$  cations and  $\text{Au}(\text{CN})_2^-$  anions as well as the relative dispositions of the  $\alpha$ -CD tori.

**Table 1. Intermolecular Distances (Å)<sup>a</sup> between  $\text{KAu}(\text{CN})_2$  and  $\alpha$ -CD in the Solid-State Superstructures with 1:1 and 1:2 Stoichiometries**

	[Au···C-5]	[Au···C-6]	[NC···C-3]	[CN···C-3]	[NC···C-5]	[CN···C-5]	[K <sup>+</sup> ···O]
$\text{Au}(\text{CN})_2^- \subset \alpha\text{-CD}^b$	4.0–4.3/5	>4.5	4.1/1	3.9–4.4/2	4.0–4.2/3	4.3–4.4/2	2.7–3.2/7
$\text{Au}(\text{CN})_2^- \subset (\alpha\text{-CD})_2^b$	>4.5	3.9–4.5/5	>4.5	>4.5	4.0–4.5/9	3.7–4.5/9	2.7–3.2/7

<sup>a</sup>These short distances suggest that the supramolecular complexes are sustained by multiple [CH···π] and [CH···anion] interactions. <sup>b</sup>The number of protons from the glucose subunits involved in short contacts (distance <4.5 Å) with  $\text{Au}(\text{CN})_2^-$  is presented after the slash symbol.

and [C–H···anion]<sup>87–90</sup> interactions between  $\text{Au}(\text{CN})_2^-$  and the inward-facing H-3, H-5, and H-6 protons. These noncovalent interactions are revealed<sup>91,92</sup> (Figure S8) by a reduced-density gradient analysis. The K<sup>+</sup> ions are located on both the primary and secondary faces of  $\alpha$ -CD. Each K<sup>+</sup> ion is linked to three  $\alpha$ -CDs with a capped trigonal prismatic coordination geometry and a coordination number of seven, two of which are involved with water molecules as ligands. Two types of K<sup>+</sup> ions are found (Figure 1c) in the packing of the crystals. Type 1 K<sup>+</sup> ions link one primary  $\alpha$ -CD face and two secondary faces, while type 2 K<sup>+</sup> ions connect one secondary face and two primary faces of the  $\alpha$ -CDs. The [K<sup>+</sup>···O] ion–dipole distances are in the range 2.7–3.2 Å. It is worth noting that the [K<sup>+</sup>···N≡C] distances are in the range 5.4–7.9 Å, suggesting the existence of relatively weak electrostatic attractions, stabilizing the adducts in the solid state. The alignment (Figure 1d and Figure S1) of  $\alpha$ -CDs is in the repeating order of HT–HH–TT where H (head) represents the secondary face and T (tail) represents the primary face of the  $\alpha$ -CDs. The HT and TT plane-to-plane distances ([O···O] from the OH groups on the opposing faces) are in the range 2.9–3.6 Å, and the HH plane-to-plane distances ([O···O] from the OH groups of the primary faces) are around 3.8 Å.

Single crystals of a 2:1 adduct were also obtained<sup>93</sup> (Figure 2) as a result of slow diffusion of EtOH into an aqueous solution containing a mixture of  $\alpha$ -CD and  $\text{KAu}(\text{CN})_2$ . The solid-state superstructure of the 2:1 adduct between  $\alpha$ -CD and  $\text{Au}(\text{CN})_2^-$  is illustrated in Figure 2. The  $\text{Au}(\text{CN})_2^-$  is located between two  $\alpha$ -CD primary faces and is tilted by about 22° relative to its principal axis (Figure 2a,b). There are nine H-5 protons from  $\alpha$ -CD in close contact (Table 1 and Table S2) with the cyanide nitrogen atoms with [C≡N···C-5] distances in the range 3.7–4.5 Å. Five of the H-6 protons in  $\alpha$ -CD have [Au···C-6] contact with the distance in the range 3.9–4.5 Å (Figure S9). The multiple [C–H···π]<sup>84–86</sup> and [C–H···anion]<sup>87–90</sup> interactions, which stabilize the 2:1 adduct between  $\alpha$ -CD and  $\text{Au}(\text{CN})_2^-$ , are associated mainly with the inward-facing H-5 and H-6 protons. Next to each of the cyanide ligands is located an EtOH molecule, forming (Figure 2c) a hydrogen bond with  $\text{Au}(\text{CN})_2^-$ . The [O···N≡C] distance was found to be 2.8 Å, suggesting the existence of strong hydrogen-bonding interactions between the EtOH molecules and  $\text{Au}(\text{CN})_2^-$ . The binding energies of  $\text{Au}(\text{CN})_2^-$  in the single-crystal superstructure were determined by DFT calculations and are shown (Table S7) to be (i) to one  $\alpha$ -CD (−42.4 kcal mol<sup>−1</sup>), (ii) to both  $\alpha$ -CDs (−79.4 kcal mol<sup>−1</sup>), (iii) to one EtOH (−12.9 kcal mol<sup>−1</sup>), (iv) to both EtOH (−22.5 kcal mol<sup>−1</sup>), (v) to one EtOH and one  $\alpha$ -CD (−62.8 kcal mol<sup>−1</sup>), and (vi) to all, that is, two  $\alpha$ -CDs and two EtOH molecules (−119.8 kcal mol<sup>−1</sup>). The EtOH molecules, which occupy part of the internal cavities of the  $\alpha$ -CDs, enhance the overall stability of the 2:1 adduct and thus facilitate the shift in the binding stoichiometry from 1:1 to 2:1. The K<sup>+</sup> ions are only found at the secondary faces of the  $\alpha$ -CDs. Each K<sup>+</sup> ion is

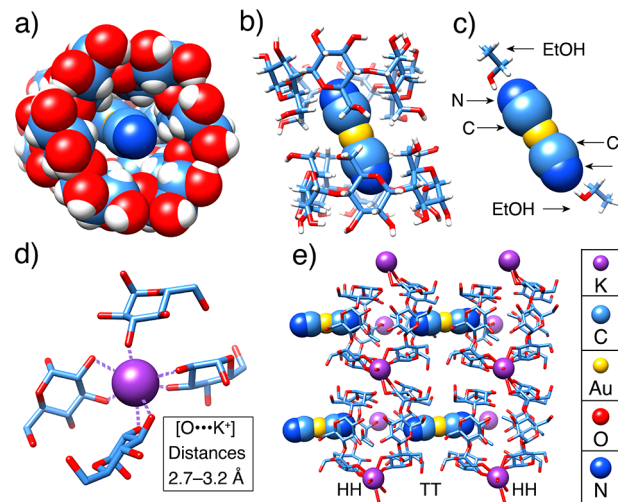


**Figure 2.** Space-filling (a) and tubular (b) representations of the solid-state superstructures of  $\text{Au}(\text{CN})_2^- \subset (\alpha\text{-CD})_2$  obtained from single-crystal X-ray diffraction studies. The inward-facing H-5 and H-6 protons of  $\alpha$ -CD are directed toward the  $\text{Au}(\text{CN})_2^-$  anion, establishing multiple [C–H···π] and [C–H···anion] interactions that stabilize the adduct. (c) Tubular representations of two EtOH molecules associated with the  $\text{Au}(\text{CN})_2^-$  anion in a space-filling representation. (d) Tubular and space-filling representations of a K<sup>+</sup> ion, forming seven [K<sup>+</sup>···O] coordinative bonds with glucose residues with a capped trigonal prismatic coordination geometry. The K<sup>+</sup> ions are only located at the secondary faces of  $\alpha$ -CDs. Each K<sup>+</sup> ion connects four  $\alpha$ -CDs together. (e) Tubular ( $\alpha$ -CD) and space-filling ( $\text{KAu}(\text{CN})_2$ ) representations of the crystal packing between  $\text{Au}(\text{CN})_2^-$  anions and  $\alpha$ -CDs, showing the position of K<sup>+</sup> cations and  $\text{Au}(\text{CN})_2^-$  anions as well as the relative disposition of the  $\alpha$ -CD tori.

linked (Figure 2d) to four  $\alpha$ -CDs with a capped trigonal prismatic coordination geometry and a coordination number of seven. The [K<sup>+</sup>···O] ion–dipole distances are in the range 2.7–3.2 Å. The relative arrangement (Figure 2e and Figure S3) of  $\alpha$ -CDs repeats in the order HH and TT with plane-to-plane distances ([O···O] from the OH groups on the opposing primary faces and secondary faces) of 2.7–3.2 and 3.8–4.1 Å, respectively.

The association between  $\alpha$ -CD and  $\text{KAu}(\text{CN})_2$  in D<sub>2</sub>O was investigated by <sup>1</sup>H NMR titrations. The resonances for H-3 and H-5 (Scheme 1) of  $\alpha$ -CD undergo downfield shifts (Figure 3a) upon titration with  $\text{KAu}(\text{CN})_2$ . In comparison, a mixture of KCl (25 mM) and  $\alpha$ -CD does not show (Figure S19) any chemical shift of the resonances for these protons, suggesting these chemical shifts are induced by the binding between  $\alpha$ -CD and the  $\text{Au}(\text{CN})_2^-$  anion. Following the chemical shift of H-3, the titration curve reveals (Figure 3b,c) a 1:1 binding stoichiometry commensurate with the solid-state superstructure obtained from the single crystal of the 1:1 adduct grown from aqueous solution. The binding constant ( $K_b$ ) between  $\text{Au}(\text{CN})_2^-$  and  $\alpha$ -CD in D<sub>2</sub>O was determined<sup>94</sup> (Figures S15–S18) to be  $8.1 \times 10^4 \text{ M}^{-1}$ .

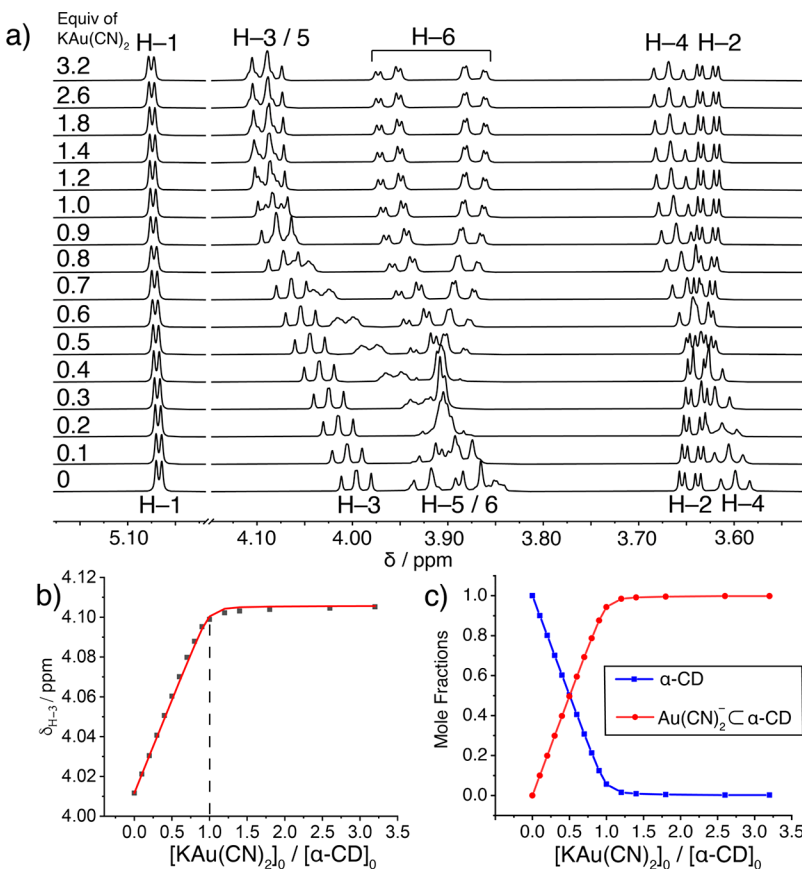


**Figure 3.** (a)  $^1\text{H}$  NMR (600 MHz,  $\text{D}_2\text{O}$ , 25  $^\circ\text{C}$ ) spectra of  $\alpha\text{-CD}$  (5 mM) titrated with  $\text{KAu}(\text{CN})_2$ . Proton numerical labels refer to the structural formula in **Scheme 1**. (b) Changes in chemical shift of H-3 caused by addition of  $\text{KAu}(\text{CN})_2$ . Red trace represents curve fitting using a 1:1 receptor–substrate binding model. (c) Calculated changes in mole fractions for  $\alpha\text{-CD}$  (blue trace) and  $\text{Au}(\text{CN})_2^- \subset \alpha\text{-CD}$  (red trace) in  $\text{D}_2\text{O}$  as a function of the substrate–receptor mole ratio, suggesting a 1:1 binding stoichiometry.

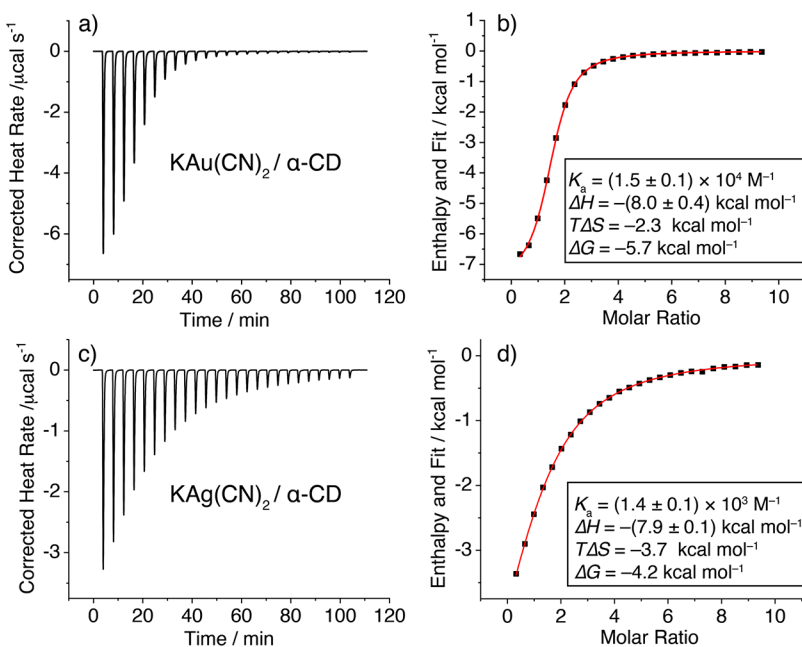


**Figure 4.** ITC Profiles for the titration of  $\text{KAu}(\text{CN})_2$  (0.5 mM, a and b) and  $\text{KAg}(\text{CN})_2$  (0.5 mM, c and d) with  $\alpha\text{-CD}$  at 25  $^\circ\text{C}$  in  $\text{H}_2\text{O}$ . The red solid line represents the best-fitting curve obtained assuming a 1:1 receptor–substrate binding model.

To shed more light on the driving force for the 1:1 adduct formation between  $\text{Au}(\text{CN})_2^-$  and  $\alpha\text{-CD}$  in water, isothermal titration calorimetry (ITC) was performed<sup>95</sup> at 25  $^\circ\text{C}$ . The

molecular recognition between  $\alpha\text{-CD}$  and  $\text{Au}(\text{CN})_2^-$  is accompanied (Figure 4a,b) by an exothermal process, where the binding enthalpy ( $\Delta H$ ) is found to be  $-8.0 \text{ kcal mol}^{-1}$ .

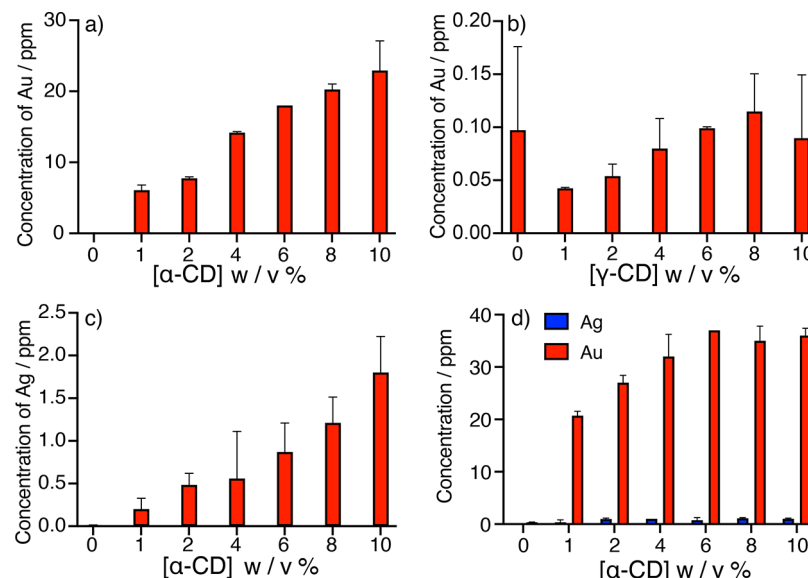


**Figure 5.** Histograms showing the average concentrations of metals stripped from the surface of activated carbon by cyclodextrins. Effect of the concentrations of (a)  $\alpha$ -CD and (b)  $\gamma$ -CD on the stripping of  $\text{KAu}(\text{CN})_2$ . (c) Effect of the concentration of  $\alpha$ -CD on the stripping of  $\text{KAg}(\text{CN})_2$  and (d) effect of the concentration of  $\alpha$ -CD on selective stripping of  $\text{KAu}(\text{CN})_2$  from a mixture of  $\text{KAu}(\text{CN})_2$  and  $\text{KAg}(\text{CN})_2$  loaded on the surface of activated carbon.

The titration curve follows a 1:1 binding model and produces a binding constant of  $1.5 \times 10^4 \text{ M}^{-1}$ . The Gibbs free energy of binding was determined to be  $-5.7 \text{ kcal mol}^{-1}$ , which allows us to deduce a binding entropy that is associated with a  $T\Delta S$  value of  $-2.3 \text{ kcal mol}^{-1}$ . These results suggest that the binding between  $\text{Au}(\text{CN})_2^-$  and  $\alpha$ -CD is driven<sup>96</sup> by a favorable enthalpy change overcoming a small entropic penalty.

The binding affinity ( $K_a = 1.4 \times 10^3 \text{ M}^{-1}$ ) between  $\text{Ag}(\text{CN})_2^-$  (Figure 4c,d) and  $\alpha$ -CD is an order of magnitude weaker compared with that of  $\text{Au}(\text{CN})_2^-$ . The binding enthalpy ( $\Delta H = -7.9 \text{ kcal mol}^{-1}$ ) of  $\text{Ag}(\text{CN})_2^-$  is similar to that of  $\text{Au}(\text{CN})_2^-$ , which is reasonable considering their similarities in size and shape. This similarity is corroborated (Table S4) by DFT calculations. The binding energy of the optimized  $\text{Au}(\text{CN})_2^- \subset \alpha\text{-CD}$  is  $-35.6 \text{ kcal mol}^{-1}$ , and that of the  $\text{Ag}(\text{CN})_2^- \subset \alpha\text{-CD}$  is  $-36.2 \text{ kcal mol}^{-1}$ .

The decrease in binding affinity of  $\alpha$ -CD for  $\text{Ag}(\text{CN})_2^-$  in  $\text{H}_2\text{O}$  is the result of a larger entropic penalty associated with a  $T\Delta S$  value of  $-3.7 \text{ kcal mol}^{-1}$ , which can be attributed to the difference in hydration states of the  $\text{Au}(\text{CN})_2^-$  and  $\text{Ag}(\text{CN})_2^-$  ions in water. This result suggests that the binding of  $\text{Au}(\text{CN})_2^-$  in water is most likely aided and abetted by hydrophobic effects,<sup>97–99</sup> which provide a favorable binding enthalpy by (i) releasing high-energy water from inside the  $\alpha$ -CDs, (ii) while reducing the entropic penalty resulting from the transfer of surface-bound water from the CDs and  $\text{Au}(\text{CN})_2^-$  anions into the bulk solution.

We have demonstrated that  $\alpha$ -CD, given a high-affinity for  $\text{Au}(\text{CN})_2^-$  anions in  $\text{H}_2\text{O}$ , can be applied as a stripping agent to remove  $\text{KAu}(\text{CN})_2$  from the surface of activated carbon at room temperature. The  $\text{KAu}(\text{CN})_2$  stripping experiments were performed at room temperature. An aqueous solution (5 mL) of  $\alpha$ -CD at a range of concentrations (1–10% w/v) was mixed (Supporting Information, section 6) with  $\text{KAu}(\text{CN})_2$ -loaded carbon (50 mg, containing 0.6 mg of gold), and the suspension was stirred for 30 min, after which time the carbon was isolated by filtration. The concentration of gold in the filtrate was determined by inductively coupled plasma mass spectrometry.

The concentration of the stripped gold increases (Figure 5a) when higher concentrations of  $\alpha$ -CD are employed. When the concentration of gold reaches 23 ppm, the corresponding  $\text{KAu}(\text{CN})_2$  recovery efficiency is 19%. As a comparison, a blank aqueous solution elutes  $<0.1$  ppm gold from the carbon, corresponding to a much lower recovery efficiency of 0.08%. In the presence of  $\alpha$ -CD, the  $\text{KAu}(\text{CN})_2$  recovery efficiency is enhanced by a factor of 237. When using  $\gamma$ -CD, a low-affinity receptor for  $\text{Au}(\text{CN})_2^-$ , we observed (Figure 5b) little enhancement of the  $\text{KAu}(\text{CN})_2$  stripping. The high affinity of  $\alpha$ -CD is crucial for the successful stripping of  $\text{KAu}(\text{CN})_2$  from the surface of activated carbon.

We have also tested  $\text{KAg}(\text{CN})_2$  stripping using the same protocol. Compared with  $\text{KAu}(\text{CN})_2$ , the recovery (Figure 5c) of  $\text{KAg}(\text{CN})_2$  is much less efficient. The highest concentration of silver stripped from the surface of activated carbon by using 10% w/v  $\alpha$ -CD is 1.8 ppm on account of the low binding affinity of  $\alpha$ -CD with  $\text{Ag}(\text{CN})_2^-$ . This result encouraged us to investigate selective  $\text{KAg}(\text{CN})_2$  stripping from the surface of activated carbon loaded with  $\text{KAu}(\text{CN})_2$  and  $\text{KAg}(\text{CN})_2$ . The concentration of stripped gold reached (Figure 5d) as high as 37 ppm, while the concentration of silver was below 1.2 ppm in all samples, suggesting a high stripping selectivity in favor of  $\text{KAu}(\text{CN})_2$ . In addition, we have noted that a higher  $\text{KAu}(\text{CN})_2$  stripping efficiency (31%) is achieved in the presence of  $\text{KAg}(\text{CN})_2$ , which could compete with  $\text{KAu}(\text{CN})_2$  on the carbon surface and promote its desorption. The high stripping selectivity of  $\text{KAu}(\text{CN})_2$  over  $\text{KAg}(\text{CN})_2$  from the surface of activated carbon could make the carbon-in-pulp process particularly attractive for gold mining with high silver-containing ores.

## CONCLUSIONS

We have reported the molecular recognition of  $\text{Au}(\text{CN})_2^-$  by  $\alpha$ -cyclodextrin in aqueous solution with a binding affinity on the order of  $10^4 \text{ M}^{-1}$ . The binding is driven by a favorable enthalpy against a small entropic penalty. The 1:1 and 2:1 adducts between  $\alpha$ -cyclodextrin and  $\text{KAu}(\text{CN})_2$  are sustained

by multiple [C–H···π] and [C–H···anion] interactions in addition to hydrophobic effects. These findings expand the scope of second-sphere coordination<sup>100–103</sup> of transition-metal complexes by  $\alpha$ -cyclodextrin beyond those already recorded in the literature<sup>104,105</sup> for (i) the neutral anticancer chemotherapeutic agent, carboplatin, (ii) the cationic [Rh(cod)-NH<sub>3</sub>)]<sup>2+</sup> as its hexafluorophosphate,<sup>106</sup> and (iii) the anionic AuBr<sub>4</sub><sup>−</sup> as its potassium salt.<sup>31,32,78,79</sup> Second-sphere coordination adducts involving  $\beta$ - and  $\gamma$ -cyclodextrins—as well as their methylated derivatives—with transition metal complexes, such as ferrocene,<sup>107</sup> [Rh(cod)Cl]<sub>2</sub>, [Pt(cod)X]<sub>2</sub> (X = Cl, Br, and I),<sup>108,109</sup> cobalt clusters,<sup>110</sup> and the neutral phosphane–transition metal complexes,<sup>111</sup> *trans*-[Pt(PR<sub>3</sub>)Cl<sub>2</sub>(NH<sub>3</sub>)] where R = Me and Et, were reported in the literature in the 1980s. It would appear that the ability of the readily available cyclodextrins and their methylated derivatives to form adducts with neutral and charged transition metal complexes in aqueous solution is wide in its scope.

We have demonstrated that the molecular recognition between  $\alpha$ -cyclodextrin and Au(CN)<sub>2</sub><sup>−</sup> can be applied to strip gold from the surface of activated carbon at room temperature. We also show that  $\alpha$ -cyclodextrin can strip selectively Au(CN)<sub>2</sub><sup>−</sup> in the presence of Ag(CN)<sub>2</sub><sup>−</sup>, a process that is difficult to achieve using the current carbon-in-pulp process. These findings could, in principle, be integrated into commercial gold-mining protocols and lead to significantly reduced costs, energy consumption, and environmental impact.

## ASSOCIATED CONTENT

### Supporting Information

The Supporting Information is available free of charge at <https://pubs.acs.org/doi/10.1021/jacs.0c11769>.

X-ray crystal data, computational investigations, binding studies by NMR spectroscopy, binding studies by isothermal titration calorimetry, and experimental procedures for gold and silver stripping ([PDF](#))

Crystallographic data for  $\alpha$ -CD·KAu(CN)<sub>2</sub> ([CIF](#))

Crystallographic data for  $(\alpha$ -CD)<sub>2</sub>·KAu(CN)<sub>2</sub> ([CIF](#))

Crystallographic data for  $(\alpha$ -CD)<sub>2</sub>·KAg(CN)<sub>2</sub> ([CIF](#))

## AUTHOR INFORMATION

### Corresponding Author

J. Fraser Stoddart — Department of Chemistry, Northwestern University, Evanston, Illinois 60208, United States; School of Chemistry, University of New South Wales, Sydney, NSW 2052, Australia;  [orcid.org/0000-0003-3161-3697](https://orcid.org/0000-0003-3161-3697); Email: [stoddart@northwestern.edu](mailto:stoddart@northwestern.edu)

### Authors

Wenqi Liu — Department of Chemistry, Northwestern University, Evanston, Illinois 60208, United States;  [orcid.org/0000-0001-6408-0204](https://orcid.org/0000-0001-6408-0204)

Leighton O. Jones — Department of Chemistry, Northwestern University, Evanston, Illinois 60208, United States;  [orcid.org/0000-0001-6657-2632](https://orcid.org/0000-0001-6657-2632)

Huang Wu — Department of Chemistry, Northwestern University, Evanston, Illinois 60208, United States;  [orcid.org/0000-0002-7429-0982](https://orcid.org/0000-0002-7429-0982)

Charlotte L. Stern — Department of Chemistry, Northwestern University, Evanston, Illinois 60208, United States

Rebecca A. Sponenborg — Quantitative Bio-Element Imaging Center, Northwestern University, Evanston, Illinois 60208, United States

George C. Schatz — Department of Chemistry, Northwestern University, Evanston, Illinois 60208, United States;  [orcid.org/0000-0001-5837-4740](https://orcid.org/0000-0001-5837-4740)

Complete contact information is available at: <https://pubs.acs.org/10.1021/jacs.0c11769>

### Notes

The authors declare the following competing financial interest(s): W. Liu and J. F. Stoddart have lodged an invention disclosure through Northwestern University based on this research entitled Supramolecular Gold Stripping from Activated Carbon Using alpha-Cyclodextrin.

## ACKNOWLEDGMENTS

We thank Professor Brad Smith at the University of Notre Dame for discussions on receptors for dicyanoaurate, which was the source of the inspiration for this work. We thank Professor Martín Mosquera at Montana State University for help with DFT calculations. We thank Northwestern University (NU) for their support of this research. This research work was also funded by the Center for Sustainable Separations of Metals (CSSM), a National Science Foundation (NSF) Center for Chemical Innovation (CCI), Grant CHE-1925708. This research was supported in part by the computational resources and staff contributions provided for the Quest High Performance Computing Facility at Northwestern University, which is jointly supported by the Office of the Provost, the Office for Research, and Northwestern University Information Technology. This work made use of the Integrated Molecular Structure Education and Research Center (IMSERC) NMR facility at Northwestern University, which has received support from the Soft and Hybrid Nanotechnology Experimental (SHyNE) Resource (NSF ECCS-2025633) and Northwestern University. Metal analysis was performed at the Northwestern University Quantitative Bio-Element Imaging Center, generously supported by NASA Ames Research Center Grants NNA04CC36G and NNA06CB93G.

## REFERENCES

- (1) *Gold Ore Processing: Project Development and Operations*; Adams, M. D., Ed.; Elsevier: Singapore, 2016.
- (2) Hutchings, G. J.; Brust, M.; Schmidbaur, H. Gold — An Introductory Perspective. *Chem. Soc. Rev.* **2008**, *37*, 1759–1765.
- (3) Gorin, D. J.; Toste, F. D. Relativistic Effects in Homogeneous Gold Catalysis. *Nature* **2007**, *446*, 395–403.
- (4) Puddephatt, R.; Macrocycles, J. Catenanes, Oligomers and Polymers in Gold Chemistry. *Chem. Soc. Rev.* **2008**, *37*, 2012–2027.
- (5) Corma, A.; Garcia, H. Supported Gold Nanoparticles as Catalysts for Organic Reactions. *Chem. Soc. Rev.* **2008**, *37*, 2096–2126.
- (6) Goldup, S. M.; Leigh, D. A.; Lusby, P. J.; McBurney, R. T.; Slawin, A. M. Z. Gold(I)-Template Catenane and Rotaxane Synthesis. *Angew. Chem., Int. Ed.* **2008**, *47*, 6999–7003.
- (7) Galli, M.; Lewis, J. E. M.; Goldup, S. M. A Stimuli-Responsive Rotaxane–Gold Catalyst: Regulation of Activity and Diastereoselectivity. *Angew. Chem., Int. Ed.* **2015**, *54*, 13545–13549.
- (8) Pflästerer, D.; Hashmi, A. S. K. Gold Catalysis in Total Synthesis — Recent Achievements. *Chem. Soc. Rev.* **2016**, *45*, 1331–1367.

(9) Lewis, J. E. M.; Beer, P. D.; Loeb, S. J.; Goldup, S. M. Metal Ions in the Synthesis of Interlocked Molecules and Materials. *Chem. Soc. Rev.* **2017**, *46*, 2577–2591.

(10) Taschinski, S.; Dopp, R.; Ackermann, M.; Rominger, F.; Vries, F.; Menger, M. F. S. J.; Rudolph, M.; Hashmi, A. S. K.; Klein, J. E. M. N. Light-Induced Mechanistic Divergence in Gold(I) Catalysis: Revisiting the Reactivity of Diazonium Salts. *Angew. Chem., Int. Ed.* **2019**, *58*, 16988–16993.

(11) Grzelczak, M.; Pérez-Juste, J.; Mulvaney, P.; Liz-Marzán, L. M. Shape Control in Gold Nanoparticle Synthesis. *Chem. Soc. Rev.* **2008**, *37*, 1783–1791.

(12) Giljohann, D. A.; Seferos, D. S.; Daniel, W. L.; Massich, M. D.; Patel, P. C.; Mirkin, C. A. Gold Nanoparticles for Biology and Medicine. *Angew. Chem., Int. Ed.* **2010**, *49*, 3280–3294.

(13) Saha, K.; Agasti, S. S.; Kim, C.; Li, X.; Rotello, V. M. Gold Nanoparticles in Chemical and Biological Sensing. *Chem. Rev.* **2012**, *112*, 2739–2779.

(14) Personick, M. L.; Mirkin, C. A. Making Sense of the Mayhem Behind Shape Control in the Synthesis of Gold Nanoparticles. *J. Am. Chem. Soc.* **2013**, *135*, 18238–18247.

(15) Bishop, P. T.; Ashfield, L. J.; Berzins, A.; Boardman, A.; Buche, V.; Cookson, J.; Gordon, R. J.; Salcianu, C.; Sutton, P. A. Printed Gold for Electronic Applications. *Gold Bull.* **2010**, *43*, 181–188.

(16) Goodman, P. Current and Future Uses of Gold in Electronics. *Gold Bull.* **2002**, *35*, 21–26.

(17) Sperling, R. A.; Rivera Gil, P.; Zhang, F.; Zanella, M.; Parak, W. J. Biological Applications of Gold Nanoparticles. *Chem. Soc. Rev.* **2008**, *37*, 1909–1930.

(18) Boisselier, E.; Astruc, D. Gold Nanoparticles in Nanomedicine: Preparations, Imaging, Diagnostics. *Chem. Soc. Rev.* **2009**, *38*, 1759–1782.

(19) Yang, Z.; Jiang, G.; Xu, Z.; Zhao, S.; Liu, W. Advances in Alkynyl Gold Complexes for Use as Potential Anticancer Agents. *Coord. Chem. Rev.* **2020**, *423*, 213492.

(20) Hilson, G.; Monhemius, A. J. Alternatives to Cyanide in the Gold Mining Industry: What Prospects for the Future? *J. Cleaner Prod.* **2006**, *14*, 1158–1167.

(21) Hagelüken, C.; Corti, C. W. Recycling of Gold from Electronics: Cost-Effective Use through “Design for Recycling”. *Gold Bull.* **2010**, *43*, 209–220.

(22) Syed, S. Recovery of Gold from Secondary Sources – A Review. *Hydrometallurgy* **2012**, *115*–*116*, 30–51.

(23) Nelson, J. J. M.; Schelter, E. J. Sustainable Inorganic Chemistry: Metal Separations for Recycling. *Inorg. Chem.* **2019**, *58*, 979–990.

(24) Rao, M. D.; Singh, K. K.; Morrison, C. A.; Love, J. B. Challenges and Opportunities in the Recovery of Gold from Electronic Waste. *RSC Adv.* **2020**, *10*, 4300–4309.

(25) Adams, M. D. The Mechanism of Adsorption of Aurocyanide onto Activated Carbon, I. Relation between the Effects of Oxygen and Ionic Strength. *Hydrometallurgy* **1990**, *25*, 171–184.

(26) Adams, M. D.; McDougall, G. J.; Hancock, R. D. Models for the Adsorption of Aurocyanide onto Activated Carbon. Part II: Extraction of Aurocyanide Ion Pairs by Polymeric Adsorbents. *Hydrometallurgy* **1987**, *18*, 139–154.

(27) Zadra, J. B. A Process for the Recovery of Gold from Activated Carbon by Leaching and Electrolysis; Report of Investigations/United States Department of the Interior, Bureau of Mines; U.S. Department of the Interior, Bureau of Mines, 1950.

(28) Ubaldini, S.; Massidda, R.; Vegliò, F.; Beolchini, F. Gold Stripping by Hydro-Alcoholic Solutions from Activated Carbon: Experimental Results and Data Analysis by a Semi-Empirical Model. *Hydrometallurgy* **2006**, *81*, 40–44.

(29) Soleimani, M.; Kaghazchi, T. Gold Recovery from Loaded Activated Carbon Using Different Solvents. *J. Chin. Inst. Chem. Eng.* **2008**, *39*, 9–11.

(30) Bunney, K.; Jeffrey, M. I.; Pleysier, R.; Breuer, P. L. Selective Elution of Gold, Silver and Mercury Cyanide from Activated Carbon. *Miner. Metall. Process.* **2010**, *27*, 205–211.

(31) Liu, Z.; Frasconi, M.; Lei, J.; Brown, Z. J.; Zhu, Z.; Cao, D.; Iehl, J.; Liu, G.; Fahrenbach, A. C.; Botros, Y. Y.; Farha, O. K.; Hupp, J. T.; Mirkin, C. A.; Fraser Stoddart, J. Selective Isolation of Gold Facilitated by Second-Sphere Coordination with  $\alpha$ -Cyclodextrin. *Nat. Commun.* **2013**, *4*, 1855.

(32) Liu, Z.; Samanta, A.; Lei, J.; Sun, J.; Wang, Y.; Stoddart, J. F. Cation-Dependent Gold Recovery with  $\alpha$ -Cyclodextrin Facilitated by Second-Sphere Coordination. *J. Am. Chem. Soc.* **2016**, *138*, 11643–11653.

(33) Fissaha, H. T.; Torrejos, R. E. C.; Kim, H.; Chung, W. J.; Nisola, G. M. Thia-Crown Ether Functionalized Mesoporous Silica (SBA-15) Adsorbent for Selective Recovery of Gold ( $\text{Au}^{3+}$ ) Ions from Electronic Waste Leachate. *Microporous Mesoporous Mater.* **2020**, *305*, 110301.

(34) Lin, R.-L.; Dong, Y.-P.; Tang, M.; Liu, Z.; Tao, Z.; Liu, J.-X. Selective Recovery and Detection of Gold with Cucurbit[n]urils ( $n = 5$ – $7$ ). *Inorg. Chem.* **2020**, *59*, 3850–3855.

(35) Chen, L.-X.; Liu, M.; Zhang, Y.-Q.; Zhu, Q.-J.; Liu, J.-X.; Zhu, B.-X.; Tao, Z. Outer Surface Interactions to Drive Cucurbit[8]uril-Based Supramolecular Frameworks: Possible Application in Gold Recovery. *Chem. Commun.* **2019**, *55*, 14271–14274.

(36) Wu, H.; Jones, L. O.; Wang, Y.; Shen, D.; Liu, Z.; Zhang, L.; Cai, K.; Jiao, Y.; Stern, C. L.; Schatz, G. C.; Stoddart, J. F. High-Efficiency Gold Recovery Using Cucurbit[6]uril. *ACS Appl. Mater. Interfaces* **2020**, *12*, 38768–38777.

(37) Serpell, C. J.; Cookson, J.; Ozkaya, D.; Beer, P. D. Core@shell Bimetallic Nanoparticle Synthesis via Anion Coordination. *Nat. Chem.* **2011**, *3*, 478–483.

(38) Wang, L.-L.; Tu, Y.-K.; Yao, H.; Jiang, W. 2,3-Dibutoxynaphthalene-Based Tetralactam Macrocycles for Recognizing Precious Metal Chloride Complexes. *Beilstein J. Org. Chem.* **2019**, *15*, 1460–1467.

(39) Doidge, E. D.; Carson, I.; Tasker, P. A.; Ellis, R. J.; Morrison, C. A.; Love, J. B. A Simple Primary Amide for the Selective Recovery of Gold from Secondary Resources. *Angew. Chem., Int. Ed.* **2016**, *55*, 12436–12439.

(40) Liu, W.; Oliver, A. G.; Smith, B. D. Macrocyclic Receptor for Precious Gold, Platinum, or Palladium Coordination Complexes. *J. Am. Chem. Soc.* **2018**, *140*, 6810–6813.

(41) Doidge, E. D.; Kinsman, L. M. M.; Ji, Y.; Carson, I.; Duffy, A. J.; Kordas, I. A.; Shao, E.; Tasker, P. A.; Ngwenya, B. T.; Morrison, C. A.; Love, J. B. Evaluation of Simple Amides in the Selective Recovery of Gold from Secondary Sources by Solvent Extraction. *ACS Sustainable Chem. Eng.* **2019**, *7*, 15019–15029.

(42) Shaffer, C. C.; Liu, W.; Oliver, A. G.; Smith, B. D. Supramolecular Paradigm for Capture and Co-Precipitation of Gold(III) Coordination Complexes. *Chem. - Eur. J.* **2020**, DOI: 10.1002/chem.202003680.

(43) Dai, Y.; Zheng, K.; Tan, Y.; Xiang, W.; Xianyu, B.; Xu, H. Fischesserite-Inspired Recyclable Se-Polyurethanes for Selective Gold Extraction. *Adv. Sustain. Syst.* **2020**, *4*, 1–6.

(44) Dong, C.-C.; Xiang, J.-F.; Xu, L.-J.; Gong, H.-Y.  $\text{MCl}_4^{n-}$  ( $\text{AuCl}_4^-$ ,  $\text{PtCl}_4^{2-}$ , or  $\text{PdCl}_4^{2-}$ ) Anion Extraction from  $\text{Na}_n\text{MCl}_4$  in Water Using a Tetraimidazolium Macrocyclic Receptor. *Tetrahedron Lett.* **2018**, *59*, 264–267.

(45) Sun, D. T.; Gasilova, N.; Yang, S.; Oveisi, E.; Queen, W. L. Rapid, Selective Extraction of Trace Amounts of Gold from Complex Water Mixtures with a Metal-Organic Framework (MOF)/Polymer Composite. *J. Am. Chem. Soc.* **2018**, *140*, 16697–16703.

(46) Zhou, S.; Hu, C.; Xu, W.; Mo, X.; Zhang, P.; Liu, Y.; Tang, K. Fast Recovery of Au (III) and Ag(I) via Amine-Modified Zeolitic Imidazolate Framework-8. *Appl. Organomet. Chem.* **2020**, *34*, e5541.

(47) Wang, C.; Lin, G.; Zhao, J.; Wang, S.; Zhang, L. Enhancing Au(III) Adsorption Capacity and Selectivity via Engineering MOF with Mercapto-1,3,4-thiadiazole. *Chem. Eng. J.* **2020**, *388*, 124221.

(48) Nguyen, T. S.; Hong, Y.; Dogan, N. A.; Yavuz, C. T. Gold Recovery from e-Waste by Porous Porphyrin–Phenazine Network Polymers. *Chem. Mater.* **2020**, *32*, 5343–5349.

(49) Ma, T.; Zhao, R.; Li, Z.; Jing, X.; Faheem, M.; Song, J.; Tian, Y.; Lv, X.; Shu, Q.; Zhu, G. Efficient Gold Recovery from e-Waste via a Chelate-Containing Porous Aromatic Framework. *ACS Appl. Mater. Interfaces* **2020**, *12*, 30474–30482.

(50) Hong, Y.; Thirion, D.; Subramanian, S.; Yoo, M.; Choi, H.; Kim, H. Y.; Stoddart, J. F.; Yavuz, C. T. Precious Metal Recovery from Electronic Waste by a Porous Porphyrin Polymer. *Proc. Natl. Acad. Sci. U. S. A.* **2020**, *117*, 16174–16180.

(51) Snowden, T. S.; Anslyn, E. V. Anion Recognition: Synthetic Receptors for Anions and Their Application in Sensors. *Curr. Opin. Chem. Biol.* **1999**, *3*, 740–746.

(52) Kubik, S. Anion Recognition in Water. *Chem. Soc. Rev.* **2010**, *39*, 3648–3663.

(53) Xu, Z.; Kim, S. K.; Yoon, J. Revisit to Imidazolium Receptors for the Recognition of Anions: Highlighted Research during 2006–2009. *Chem. Soc. Rev.* **2010**, *39*, 1457–1466.

(54) Brotherhood, P. R.; Davis, A. P. Steroid-Based Anion Receptors and Transporters. *Chem. Soc. Rev.* **2010**, *39*, 3633–3647.

(55) Busschaert, N.; Caltagirone, C.; Van Rossom, W.; Gale, P. A. Applications of Supramolecular Anion Recognition. *Chem. Rev.* **2015**, *115*, 8038–8155.

(56) Flood, A. H. Creating Molecular Macrocycles for Anion Recognition. *Beilstein J. Org. Chem.* **2016**, *12*, 611–627.

(57) Liu, Y.; Sengupta, A.; Raghavachari, K.; Flood, A. H. Anion Binding in Solution: Beyond the Electrostatic Regime. *Chem.* **2017**, *3*, 411–427.

(58) Kubik, S. Anion Recognition in Aqueous Media by Cyclopeptides and Other Synthetic Receptors. *Acc. Chem. Res.* **2017**, *50*, 2870–2878.

(59) He, Q.; Tu, P.; Sessler, J. L. Supramolecular Chemistry of Anionic Dimers, Trimers, Tetramers, and Clusters. *Chem.* **2018**, *4*, 46–93.

(60) He, Q.; Vargas-Zúñiga, G. I.; Kim, S. H.; Kim, S. K.; Sessler, J. L. Macrocycles as Ion Pair Receptors. *Chem. Rev.* **2019**, *119*, 9753–9835.

(61) Chen, L.; Berry, S. N.; Wu, X.; Howe, E. N. W.; Gale, P. A. Advances in Anion Receptor Chemistry. *Chem.* **2020**, *6*, 61–141.

(62) Hein, R.; Beer, P. D.; Davis, J. J. Electrochemical Anion Sensing: Supramolecular Approaches. *Chem. Rev.* **2020**, *120*, 1888–1935.

(63) Wang, D.-X.; Wang, M.-X. Exploring Anion–π Interactions and Their Applications in Supramolecular Chemistry. *Acc. Chem. Res.* **2020**, *53*, 1364–1380.

(64) Pancholi, J.; Beer, P. D. Halogen Bonding Motifs for Anion Recognition. *Coord. Chem. Rev.* **2020**, *416*, 213281.

(65) Wu, X.; Gilchrist, A. M.; Gale, P. A. Prospects and Challenges in Anion Recognition and Transport. *Chem.* **2020**, *6*, 1296–1309.

(66) Canumalla, A. J.; Schraa, S.; Isab, A. A.; Shaw, C. F.; Gleichmann, E.; Dunemann, L.; Turfeld, M. Equilibrium Binding Constants and Facile Dissociation of Novel Serum Albumin-Dicyanoaurate(I) Complexes. *J. Biol. Inorg. Chem.* **1998**, *3*, 9–17.

(67) Pham, D. M.; Rios, D.; Olmstead, M. M.; Balch, A. L. Assisted Self-Association of Dicyanoaurate,  $[\text{Au}(\text{CN})_2]^-$ , and Dicyanoargenate,  $[\text{Ag}(\text{CN})_2]^-$ , Through Hydrogen Bonding to Metal Ammonia Complexes. *Inorg. Chim. Acta* **2005**, *358*, 4261–4269.

(68) Moriuchi, T.; Yoshii, K.; Katano, C.; Hirao, T. Luminescent Properties of Dicyanoaurate(I) Aggregates Based on Electrostatic Assembly along Poly(allylamine hydrochloride). *Tetrahedron Lett.* **2010**, *51*, 4030–4032.

(69) Meng, W.; Clegg, J. K.; Nitschke, J. R. Transformative Binding and Release of Gold Guests from a Self-Assembled  $\text{Cu}_8\text{L}_4$  Tube. *Angew. Chem., Int. Ed.* **2012**, *51*, 1881–1884.

(70) Meng, W.; League, A. B.; Ronson, T. K.; Clegg, J. K.; Isley, W. C.; Semrouni, D.; Gagliardi, L.; Cramer, C. J.; Nitschke, J. R. Empirical and Theoretical Insights into the Structural Features and Host-Guest Chemistry of  $\text{M}_8\text{L}_4$  Tube Architectures. *J. Am. Chem. Soc.* **2014**, *136*, 3972–3980.

(71) Christopherson, J. C.; Potts, K. P.; Bushuyev, O. S.; Topić, F.; Huskić, I.; Rissanen, K.; Barrett, C. J.; Friščić, T. Assembly and Dichroism of a Four-Component Halogen-Bonded Metal-Organic Cocrystal Salt Solvate Involving Dicyanoaurate(I) Acceptors. *Faraday Discuss.* **2017**, *203*, 441–457.

(72) Andersen, N. N.; Eriksen, K.; Lisbjerg, M.; Ottesen, M. E.; Milhøj, B. O.; Sauer, S. P. A.; Pittelkow, M. Entropy/Enthalpy Compensation in Anion Binding: Biotin[6]uril and Biotin-1-sulfoxide-[6]uril Reveal Strong Solvent Dependency. *J. Org. Chem.* **2019**, *84*, 2577–2584.

(73) Villiers, A. Sur la Fermentation de la Féculle Par l’Action du Ferment Butyrique. *C. R. Hebd. Séances Acad. Sci.* **1891**, *112*, 536.

(74) Stoddart, J. F. A Century of Cyclodextrins. *Carbohydr. Res.* **1989**, *192*, 12–15.

(75) Szejtli, J. Past, Present and Future of Cyclodextrin Research. *Pure Appl. Chem.* **2004**, *76*, 1825–1845.

(76) Crini, G. Review: A History of Cyclodextrins. *Chem. Rev.* **2014**, *114*, 10940–10975.

(77) Smaldone, R. A.; Forgan, R. S.; Furukawa, H.; Gassensmith, J. J.; Slawin, A. M. Z.; Yaghi, O. M.; Stoddart, J. F. Metal–Organic Frameworks from Edible Natural Products. *Angew. Chem., Int. Ed.* **2010**, *49*, 8630–8634.

(78) Liu, Z.; Stoddart, J. F. Extended Metal-Carbohydrate Frameworks. *Pure Appl. Chem.* **2014**, *86*, 1323–1334.

(79) Liu, Z.; Schneebeli, S. T.; Stoddart, J. F. Second-Sphere Coordination Revisited. *Chimia* **2014**, *68*, 315–320.

(80) Harada, A.; Li, J.; Kamachi, M. The Molecular Necklace: A Rotaxane Containing Many Threaded  $\alpha$ -Cyclodextrins. *Nature* **1992**, *356*, 325–327.

(81) Noltemeyer, M.; Saenger, W. X-Ray Studies of Linear Polyiodide Chains in  $\alpha$ -Cyclodextrin Channels and a Model for the Starch-Iodine Complex. *Nature* **1976**, *259*, 629–632.

(82) Noltemeyer, M.; Saenger, W. Topography of Cyclodextrin Inclusion Complexes. 12. Structural Chemistry of Linear  $\alpha$ -Cyclodextrin-Polyiodide Complexes. X-Ray Crystal Structures of  $(\alpha\text{-Cyclodextrin})_2\text{-LiI}_3\text{-I}_2\text{-}8\text{H}_2\text{O}$  and  $(\alpha\text{-Cyclodextrin})_2\text{-Cd}_{0.5}\text{-I}_5\text{-}27\text{H}_2\text{O}$ . Models for the Blue Amylose-Iodide Complex. *J. Am. Chem. Soc.* **1980**, *102*, 2710–2722.

(83) We note that  $\alpha$ -CD (100 mM) requires heat for it to dissolve in  $\text{H}_2\text{O}$ . In the presence of  $\text{KAu}(\text{CN})_2$ ,  $\alpha$ -CD dissolves instantly, suggesting that complexation is occurring.

(84) Spiwok, V. CH/π Interactions in Carbohydrate Recognition. *Molecules* **2017**, *22*, 1–11.

(85) Nishio, M.; Umezawa, Y.; Fantini, J.; Weiss, M. S.; Chakrabarti, P. CH–π Hydrogen Bonds in Biological Macromolecules. *Phys. Chem. Chem. Phys.* **2014**, *16*, 12648–12683.

(86) Nishio, M. The CH/π Hydrogen Bond in Chemistry. Conformation, Supramolecules, Optical Resolution and Interactions Involving Carbohydrates. *Phys. Chem. Chem. Phys.* **2011**, *13*, 13873–13900.

(87) Ilioudis, C. A.; Tocher, D. A.; Steed, J. W. A Highly Efficient, Preorganized Macrocyclic Receptor for Halides Based on CH··· and NH···Anion Interactions. *J. Am. Chem. Soc.* **2004**, *126*, 12395–12402.

(88) Vega, I. E. D.; Gale, P. A.; Light, M. E.; Loeb, S. J. NH vs. CH Hydrogen Bond Formation in Metal-Organic Anion Receptors Containing Pyrrolylpyridine Ligands. *Chem. Commun.* **2005**, *39*, 4913–4915.

(89) Pedzisa, L.; Hay, B. P. Aliphatic C–H···Anion Hydrogen Bonds: Weak Contacts or Strong Interactions? *J. Org. Chem.* **2009**, *74*, 2554–2560.

(90) Lisbjerg, M.; Valkenier, H.; Jessen, B. M.; Al-Kerdi, H.; Davis, A. P.; Pittelkow, M. Biotin[6]uril Esters: Chloride-Selective Transmembrane Anion Carriers Employing C–H···Anion Interactions. *J. Am. Chem. Soc.* **2015**, *137*, 4948–4951.

(91) Lefebvre, C.; Rubez, G.; Khatabil, H.; Boisson, J. C.; Contreras-García, J.; Hénon, E. Accurately Extracting the Signature of Intermolecular Interactions Present in the NCI Plot of the Reduced Density Gradient versus Electron Density. *Phys. Chem. Chem. Phys.* **2017**, *19*, 17928–17936.

(92) Lu, T.; Chen, F. Multiwfn: A Multifunctional Wavefunction Analyzer. *J. Comput. Chem.* **2012**, *33*, 580–592.

(93) Under the same conditions, we obtained (Figure S5) the X-ray crystal superstructure of a 2:1 adduct between  $\alpha$ -CD and  $\text{KAg}(\text{CN})_2$ . It is worth noting that  $\text{KAg}(\text{CN})_2$  is a byproduct in the cyanide-based, gold-mining process. The adduct has an identical superstructure with the 2:1 adduct between  $\alpha$ -CD and  $\text{KAu}(\text{CN})_2$ . The two crystal superstructures are isostructural, suggesting the high similarity in superstructures and properties between these two 2:1 adducts.

(94) The titrations for  $\beta$ - and  $\gamma$ -CD using  $\text{Au}(\text{CN})_2^-$  reveal (Figures S20–S25) much weaker binding affinities in  $\text{D}_2\text{O}$  with  $K_a$  values on the order of  $10^2$  and  $10^1 \text{ M}^{-1}$ , respectively. It is worth noting that the titration data for  $\beta$ - and  $\gamma$ -CD fit poorly when using a 1:1 binding model. A 1:2 binding model between the larger CDs and  $\text{Au}(\text{CN})_2^-$  leads to a better fit, suggesting that these larger CDs can encapsulate two  $\text{Au}(\text{CN})_2^-$  ions in  $\text{D}_2\text{O}$ .

(95) A stock aqueous solution of  $\alpha$ -CD in a syringe was titrated into an aqueous solution of  $\text{KAu}(\text{CN})_2$  (0.5 mM) placed in a titration cell.

(96) 2:1 binding models were used for the data fitting, resulting in  $K_a$  values on the order of  $10^2$  and  $10^1 \text{ M}^{-1}$  for  $\beta$ - and  $\gamma$ -CD, respectively, matching the results obtained from  $^1\text{H}$  NMR titration experiments. The binding affinities of  $\text{KAu}(\text{CN})_2$  with  $\beta$ - and  $\gamma$ -CD are much weaker and fit poorly to isotherms employing (Figures S26–S29) 1:1 binding models.

(97) Biedermann, F.; Nau, W. M.; Schneider, H. J. The Hydrophobic Effect Revisited – Studies with Supramolecular Complexes Imply High-Energy Water as a Noncovalent Driving Force. *Angew. Chem., Int. Ed.* **2014**, *53*, 11158–11171.

(98) Snyder, P. W.; Lockett, M. R.; Moustakas, D. T.; Whitesides, G. M. Is It the Shape of the Cavity, or the Shape of the Water in the Cavity? *Eur. Phys. J.: Spec. Top.* **2014**, *223*, 853–891.

(99) Hillyer, M. B.; Gibb, B. C. Molecular Shape and the Hydrophobic Effect. *Annu. Rev. Phys. Chem.* **2016**, *67*, 307–329.

(100) Colquhoun, H. M.; Stoddart, J. F.; Williams, D. J. Second-Sphere Coordination—A Novel Role for Molecular Receptors. *Angew. Chem., Int. Ed. Engl.* **1986**, *25*, 487–507.

(101) Alston, D. R.; Ashton, P. R.; Lilley, T. H.; Fraser Stoddart, J.; Zarzycki, R.; Slawin, A. M. Z.; Williams, D. J. Second-Sphere Coordination of Carboplatin and Rhodium Complexes by Cyclodextrins (Cyclomalto-oligosaccharides). *Carbohydr. Res.* **1989**, *192*, 259–281.

(102) Raymo, F. M.; Stoddart, J. F. Second-Sphere Coordination. *Chem. Ber.* **1996**, *129*, 981–990.

(103) Cotton, F. A.; Wilkinson, G.; Murillo, C. A.; Bochmann, M. *Advanced Inorganic Chemistry*, 6th ed.; John Wiley & Sons, Inc.: New York, 1999; p 479.

(104) Alston, D. R.; Lilley, T. H.; Stoddart, J. F. The Binding of Cyclobutane-1,1-Dicarboxylatodiammineplatinum(II) by Alpha-Cyclodextrin in Aqueous Solution. *J. Chem. Soc., Chem. Commun.* **1985**, *22*, 1600–1602.

(105) Alston, D. R.; Slawin, A. M. Z.; Stoddart, J. F.; Williams, D. J. The X-Ray Crystal Structure of a 1:1 Adduct between  $\alpha$ -Cyclodextrin and Cyclobutane-1,1-Dicarboxylatodiammineplatinum(II). *J. Chem. Soc., Chem. Commun.* **1985**, *22*, 1602–1604.

(106) Alston, D. R.; Slawin, A. M. Z.; Stoddart, J. F.; Williams, D. J. Cyclodextrins as Second Sphere Ligands for Transition Metal Complexes—The X-Ray Crystal Structure of  $[\text{Rh}(\text{Cod})(\text{NH}_3)_2 \cdot \alpha\text{-cyclodextrin}] [\text{PF}_6^-] \cdot 6\text{H}_2\text{O}$ . *Angew. Chem., Int. Ed. Engl.* **1985**, *24*, 786–787.

(107) Harada, A.; Takahashi, S. Preparation and Properties of Cyclodextrin Inclusion Compounds of Organometallic Complexes. Ferrocene Inclusion Compounds. *J. Chem. Soc., Chem. Commun.* **1984**, *645*–646.

(108) Harada, A.; Takahashi, S. Preparation and Properties of Inclusion Compounds of Transition Metal Complexes of Cyclo-octa-1,5-diene and Norbornadiene with Cyclodextrins. *J. Chem. Soc., Chem. Commun.* **1986**, *1229*–1230.

(109) Harada, A.; Yamamoto, S.; Takahashi, S. Preparation and Properties of Inclusion Compounds of Transition-Metal Complexes of Cycloocta-1,5-diene and Norbornadiene with Cyclodextrins. *Organometallics* **1989**, *8*, 2560–2563.

(110) Harada, A.; Shimada, M.; Takahashi, S.  $\gamma$ -Cyclodextrin as a Second Sphere Coordination Ligand for Cobalt Cluster Complexes. *Chem. Lett.* **1989**, *18*, 275–276.

(111) Alston, D. R.; Slawin, A. M. Z.; Stoddart, J. F.; Williams, D. J.; Zarzycki, R. Second Sphere Coordination Adducts of Phosphane-Transition Metal Complexes with  $\beta$ -Cyclodextrin and Its Methylated Derivative. *Angew. Chem., Int. Ed. Engl.* **1988**, *27*, 1184–1185.